

1 Article

## 2 Synthesis and Antiviral Activity of Novel Myricetin 3 Derivatives Containing a Ferulic Acid Amide Scaffolds

4 Xu Tang<sup>1,†</sup>, Cheng Zhang<sup>1,†</sup>, Mei Chen<sup>1</sup>, Yining Xue<sup>2</sup>, Tingting Liu<sup>1</sup>, Wei Xue<sup>1,\*</sup>5 <sup>1</sup>State Key Laboratory Breeding Base of Green Pesticide and Agricultural Bioengineering, Key Laboratory of  
6 Green Pesticide and Agriculture Bioengineering, Ministry of Education, Guizhou University, Huaxi District,  
7 Guiyang 550025, P.R. China.8 <sup>2</sup>College of Chemistry, Chemical Engineering and Environment, Minnan Normal University, Zhangzhou  
9 363000, P.R. China.10 E-Mails: tx1173182020@163.com (X. T.); zhangcheng6954@163.com (C. Z.); 18208697744@163.com (M. C.);  
11 iotai@163.com (Y. X.); ltt15642332007@163.com (T. L).12 <sup>†</sup> These authors contributed equally to this work.13 <sup>\*</sup> Corresponding author: Wei Xue; e-mail: wxue@gzu.edu.cn (W. X.); Tel/Fax: 0086-851-88292090

14

15 **Abstract:** A variety of myricetin derivatives bearing ferulic acid amide scaffolds were designed and  
16 synthesized. The structures of all title compounds were determined by <sup>1</sup>H NMR, <sup>13</sup>C NMR, <sup>19</sup>F  
17 NMR and HRMS. Preliminary bioassays suggested that some of the target compounds exhibited  
18 remarkable antiviral activities. In particular, compound **4I** possessed significant protection activity  
19 against tobacco mosaic virus (TMV), with an half maximal effective concentration (EC<sub>50</sub>) value of  
20 196.11 μg/mL, which was better than commercial agent ningnamycin (447.92 μg/mL). Meanwhile,  
21 microscale thermophoresis (MST) indicated that compound **4I** have strong binding capability to  
22 tobacco mosaic virus coat protein (TMV-CP) with dissociation constant (K<sub>d</sub>) values of 0.34 μmol/L,  
23 which was better than ningnamycin (0.52 μmol/L). These results suggest that novel myricetin  
24 derivatives bearing ferulic acid amide scaffolds may be considered as an activator for antiviral  
25 agents.

26 Keywords: myricetin; ferulic acid; antiviral activity; microscale thermophoresis; molecular docking

27

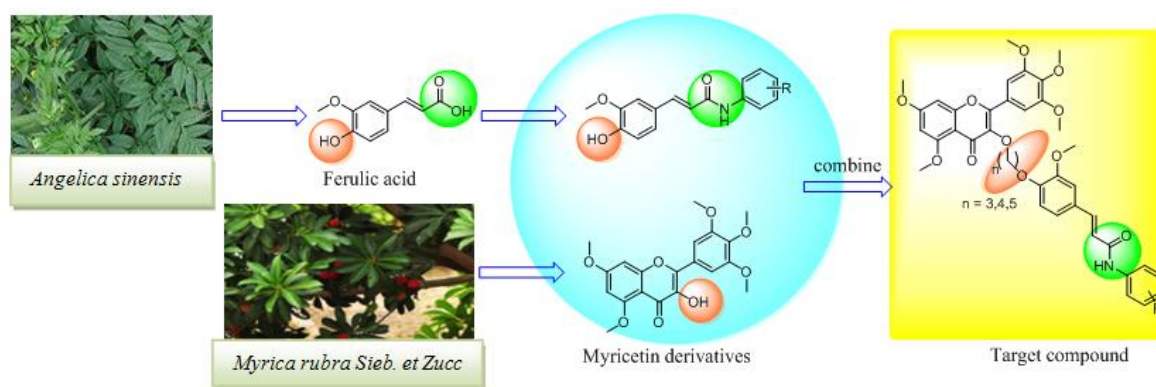
28 **1. Introduction**

29 Plant disease result in economic loss and decreases in the quality and quantity of agricultural  
30 products around the world, such as tobacco mosaic virus (TMV), it can easily infect economic crops,  
31 resulting in economic losses, people are obliged to spend millions of dollar to prevention and  
32 quarantines it [1]. Unfortunately, traditional pesticide, such as ningnanmycin and ribavirin due to its  
33 poor efficiency, high phytotoxicity, environment damage, pesticide residue and can even develop  
34 resistant from pesticide, have been eliminated and banned gradually [2, 3]. It is an urgent need to  
35 develop more greener and high-efficient promising pesticide to control and prevent plant disease.

36 Due to its low toxicity, easy decomposition, novel structure and environmental friendliness,  
37 natural products are devoted to synthesis new pesticides [4-6]. Myricetin is a kind of natural product  
38 which can extracted from several medicinal plant organs, vegetables and fruits [7], such as *myrica*

39 *rubra* Sieb [8], *Abelmoschus manihot* [9] and *onions* [10]. Literature survey revealed that myricetin has  
 40 various biological activities, like antiviral [11, 12], antibacterial [13, 14], antioxidant [15], anticancer  
 41 [16, 17] and so on. In our previous study, we have reported a series of myricetin derivatives with  
 42 appreciable bioactivities against TMV [11].

43 Ferulic acid is a phenolic acid present in many plants, such as *Angelica sinensis*, *Cimicifuga*  
 44 *heracleifolia* and *Lignsticum chuangxiong* [18]. According to reports, ferulic acid exhibits a wide range  
 45 of bioactivities, such as antiviral [19], antibacterial [20], anticancer [21, 22] and  
 46 attracted wide publicity in field of medicinal chemistry. In the further development of antiviral  
 47 agents, a series of novel myricetin derivatives containing a 1,3,4-thiadiazole moiety was found to  
 48 have excellent anti-TMV activity[12]. In this study, we aimed to use a ferulic acid amide to replace  
 49 the 1,3,4-thiadiazole system to build novel myricetin derivatives containing a ferulic acid amide  
 50 moiety for the development of antiviral agents. The preliminary bioassay results indicated that  
 51 some of target compounds showed excellent antiviral activity, Among them, compound **4l**  
 52 possessed significant protection activity against TMV. Meanwhile, MST and molecular docking  
 53 indicated that compound **4l** have strong binding capability to TMV-CP. To the best of our  
 54 knowledge, this is the first report on the synthesis and antiviral activity evaluation of myricetin  
 55 derivatives containing a ferulic acid amide moiety (**Figure 1**).



56

57 **Figure 1.** Design of novel myricetin derivatives containing ferulic acid amide scaffolds

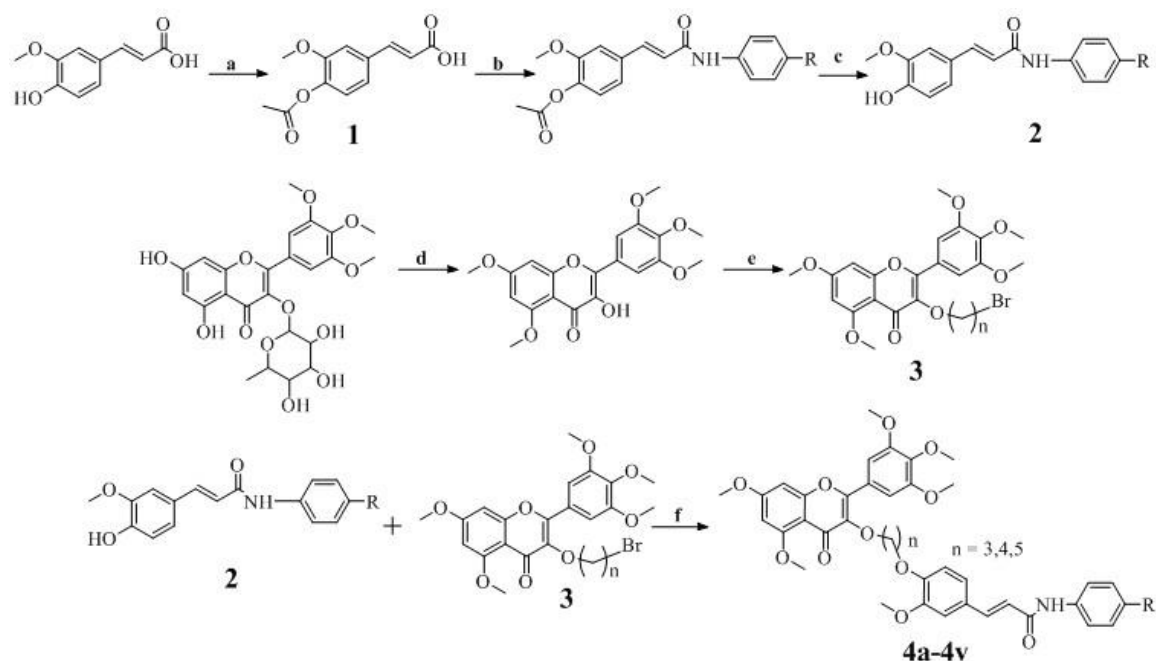
## 58 2. Results and Discussion

### 59 2.1. Chemistry

60 A synthetic route to myricetin derivatives containing ferulic acid amide scaffolds was designed  
 61 and was shown in **Scheme 1**. According to previously reported methods [16, 23], (*E*)-3-(4-acetoxy  
 62 -3-methoxyphenyl)acrylic acid (intermediate **1**) and 3-(bromomethoxy)-5,7-dimethoxy-2-(3,4,5-  
 63 trimethoxy phenyl)-4*H*-chromen-4-one (intermediate **3**) could be obtained. The (*E*)-3-(4-hydroxy-  
 64 3-methoxyphenyl)-*N*-(substituted-phenyl) acryl amide intermediate **2** were prepared from  
 65 substituted aniline and hydrazine hydrate by reported procedures [19, 24]. Finally, the title  
 66 compounds **4a-4v** were synthesized by intermediates **2** and intermediates **3** in the  $K_2CO_3$  and DMF  
 67 at reflux for 5-7 h.

68 The structures of all title compounds were determined by  $^1H$  NMR,  $^{13}C$  NMR,  $^{19}F$  NMR and  
 69 HRMS, and the spectra data were shown in the Supplementary Materials. The data of **4a** was  
 70 shown and discussed below. In the  $^1H$  NMR, multiplet signals at  $\delta$  8.01–6.36 ppm revealed the

71 presence of nitrogen hydrogen bond, protons in olefinic bonds and aromatic nuclei, and triplet  
 72 singlets at  $\delta$  4.23 and 4.18 ppm indicate the presence of  $-\text{CH}_2-$  group. In addition, the four  
 73 high-frequency single peaks and doublets peaks at 3.94-3.77 ppm revealed the presence of five  
 74  $-\text{OCH}_3$ , and double peak at  $\delta$  2.31 ppm indicate the presence of  $-\text{CH}_3$  groups. Absorption signals at  
 75  $\delta$  174.07, 164.12 and 20.91 ppm in  $^{13}\text{C}$  NMR spectra confirm the presences of  $-\text{C}=\text{O}$ ,  $-\text{C}=\text{O}-\text{NH}-$   
 76 and  $-\text{CH}_3$  groups, respectively. The high-resolution mass spectrometry (HRMS) spectra of title  
 77 compounds show characteristic absorption signals of  $[\text{M} + \text{H}]^+$  ions, which is consistent with their  
 78 molecular weight.



reaction condition: **a** : acetic anhydride, 5%NaOH; **b** : R-PhNH<sub>2</sub>, HOBt, EDCl; **c** :NH<sub>2</sub>NH<sub>2</sub>H<sub>2</sub>O, CH<sub>3</sub>CN;  
**d** : DMF, K<sub>2</sub>CO<sub>3</sub>, CH<sub>3</sub>I, cone HCl; **e** :DMF, Br(CH<sub>2</sub>CH<sub>2</sub>)<sub>n</sub>Br; **f** : DMF, K<sub>2</sub>CO<sub>3</sub>

**4a** : R = 4-CH<sub>3</sub>, n = 3; **4b** : R = 4-OCH<sub>3</sub>, n = 3; **4c** : R = 4-CH<sub>3</sub>, n = 4; **4d** : R = 4-OCH<sub>3</sub>, n = 4;  
**4e** : R = 3-Cl, n = 3; **4f** : R = 3-Cl, n = 4; **4g** : R = 4-Cl, n = 4; **4h** : R = H, n = 4;  
**4i** : R = H, n = 3; **4j** : R = 3,4-di-CH<sub>3</sub>, n = 3; **4k** : R = 3,4-di-CH<sub>3</sub>, n = 4; **4l** : R = 3,4-di-OCH<sub>3</sub>, n = 3;  
**4m** : R = 3,4-di-OCH<sub>3</sub>, n = 4; **4n** : R = 4-Br, n = 3; **4o** : R = 4-Br, n = 4; **4p** : R = 3,4-di-Cl, n = 3;  
**4q** : R = 3,4-di-Cl, n = 4; **4r** : R = 4-Cl, n = 5; **4s** : R = 3-Cl, n = 5; **4t** : R = 4-OCH<sub>3</sub>, n = 5;  
**4u** : R = 2-F, n = 3; **4v** : R = 2-F, n = 4

79

80

**Scheme 1.** Synthesis of the title compounds **4a-4v**.

## 81 2.2. Antiviral activity of title compounds against TMV *in vivo*

82 Using *N. tabacum* L. leaves under the same age as that of test subjects, the curative and  
 83 protective activities against TMV (*in vivo*) at a concentration of 500  $\mu\text{g}/\text{mL}$  were evaluated by the  
 84 half-leaf blight spot methods [25, 26], and the obtained results were shown in **Table 1**. The  
 85 preliminary bioassay results indicated that the inhibitory rates of target compounds (**4a-4v**) against  
 86 TMV ranged from 15.8 to 55.5 % in terms of their curative activities, while their protective activities  
 87 ranged from 5.3 to 62.1 %. Especially, compound **4n** showed 55.5 % curative effects at 500  $\mu\text{g}/\text{mL}$ ,  
 88 which was better than that of myricetin (35.7 %) and ningnanmycin (53.2 %). In addition,  
 89 compound **4l** exhibited significant protective activities against TMV at 500  $\mu\text{g}/\text{mL}$ , the inhibition  
 90 rate was 62.1 %, which was even better than that of myricetin (41.5 %) and ningnanmycin (55.7 %).

91  
92**Table 1** Inhibition effect (%) of the compounds **4a–4v** against TMV <sup>a</sup>

Compounds	R	n	Curative Activity (%)	Protection Activity (%)
<b>4a</b>	4-CH <sub>3</sub>	3	33.0	11.6
<b>4b</b>	4-OCH <sub>3</sub>	3	42.1	35.6
<b>4c</b>	4-CH <sub>3</sub>	4	39.6	21.2
<b>4d</b>	4-OCH <sub>3</sub>	4	15.8	5.3
<b>4e</b>	3-Cl	3	37.5	51.6
<b>4f</b>	3-Cl	4	32.1	52.3
<b>4g</b>	4-Cl	4	38.1	40.3
<b>4h</b>	H	4	41.3	48.5
<b>4i</b>	H	3	43.5	31.2
<b>4j</b>	3,4-di-CH <sub>3</sub>	3	39.4	46.4
<b>4k</b>	3,4-di-CH <sub>3</sub>	4	21.1	25.9
<b>4l</b>	3,4-di-OCH <sub>3</sub>	3	37.4	62.1
<b>4m</b>	3,4-di-OCH <sub>3</sub>	4	31.2	13.5
<b>4n</b>	4-Br	3	55.5	53.3
<b>4o</b>	4-Br	4	28.4	19.5
<b>4p</b>	3,4-di-Cl	3	37.2	58.1
<b>4q</b>	3,4-di-Cl	4	34.2	43.9
<b>4r</b>	4-Cl	5	40.4	44.1
<b>4s</b>	3-Cl	5	43.2	37.8
<b>4t</b>	4-OCH <sub>3</sub>	5	39.9	24.1
<b>4u</b>	2-F	3	37.0	41.1
<b>4v</b>	2-F	4	21.8	32.5
<b>MY</b> <sup>b</sup>	-	-	35.7	41.5
<b>NNM</b> <sup>c</sup>	-	-	53.2	55.7

93  
94

<sup>a</sup> Average of three replicates; <sup>b</sup> The lead compound of myricetin; <sup>c</sup> The commercial antirotovirics (NNM, ningnamycin) was used for comparison of antiviral activity.

95 To confirm the potential inhibitory capacity of these compounds against TMV, on the basis of  
96 our preliminary bioassay, we further evaluated the EC<sub>50</sub> of some title compounds against TMV.  
97 As shown in **Table 2**, compounds **4l**, **4n** and **4p** exhibits excellent protection activities against TMV  
98 with the EC<sub>50</sub> values of 196.1, 425.3 and 386.7 μg/mL respectively, which were superior to  
99 ningnamycin (447.9 μg/mL). Compound **4n** shows good curative activity against TMV the EC<sub>50</sub>  
100 value is 472.4 μg/mL, which was near to ningnamycin (428.8 μg/mL).

101

**Table 2** The EC<sub>50</sub> values of **4l**, **4n** and **4p** against TMV <sup>a</sup>

	Compounds	R	n	Toxic regression equation	r	EC <sub>50</sub> μg/mL
Curative Activity (%)	<b>4n</b>	4-Br	3	y=1.4582x+1.1002	0.9902	472.4
	<b>NNM</b> <sup>b</sup>	-	-	y=0.7650x+2.9863	0.9830	428.8
Protection Activity(%)	<b>4l</b>	3,4-di-OCH <sub>3</sub>	3	y=2.0488x-0.3031	0.9891	196.1
	<b>4n</b>	4-Br	3	y=1.7099x+1.7002	0.9888	425.3
	<b>4p</b>	3,4-di-Cl	3	y=1.4133x+2.3311	0.9970	386.7
	<b>NNM</b> <sup>b</sup>	-	-	y=1.5482x+0.8954	0.9819	447.9

102  
103

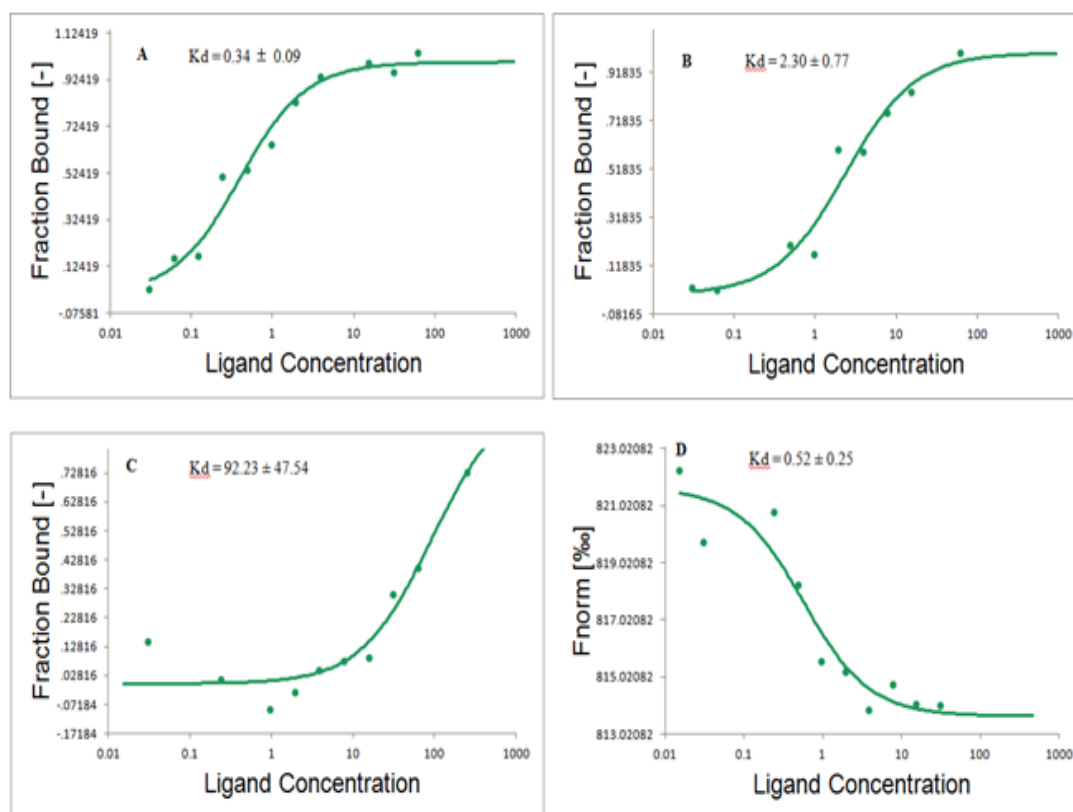
<sup>a</sup> Average of three replicates; <sup>b</sup> The commercial antirotovirics (NNM, ningnamycin) was used for comparison of antiviral activity.

### 104 2.3. Structure activity relationship (SAR) of the title compounds against TMV

105 As indicated in **Tables 1** and **2**, the antiviral effects of target compounds were greatly affected  
 106 by structural variations. Some structure–activity relationships (SAR) analyses were discussed as  
 107 below. The presence of 4-Br, 3-Cl, 4-OCH<sub>3</sub> and H groups at the R position greatly increased the  
 108 curative activities of the target compounds against TMV. For instance, the target compounds  
 109 **4b**(4-OCH<sub>3</sub>, n=3), **4i** (H, n=3), **4n** (4-Br, n=3) and **4s** (3-Cl, n=5) showed important antiviral  
 110 activities against TMV, with inhibition rates of 42.1, 43.5, 55.5 and 43.2 %, respectively.  
 111 Furthermore, when R was 3-Cl, 3,4-di-OCH<sub>3</sub> and 3,4-di-Cl groups, the protective activities of the  
 112 relevant compounds **4f**, **4l** and **4p** at 500 µg/mL were 52.3, 62.1, and 58.1 %, respectively, which were  
 113 superior to other substituent groups.

### 114 2.4. Binding sites of **4l**, **4m**, myricetin and ningnanmycin to TMV-CP

115 To further analyze the interactions between the compounds **4l**, **4m**, myricetin and  
 116 ningnanmycin and TMV-CP, MST analysis was used [27-29]. The MST results as summarized in  
 117 **Figure 2** and **Table 3** indicated that the binding of compounds **4l**, **4m**, myricetin and ningnanmycin  
 118 to TMV-CP protein yielded K<sub>d</sub> values of 0.34 ± 0.09 µmol/L, 2.30 ± 0.77 µmol/L, 92.23 ± 47.54 µmol/L  
 119 and 0.52 ± 0.25 µmol/L, respectively. As showed in MST, compound **4l** (K<sub>d</sub>=0.34 ± 0.09 µmol/L) share  
 120 strong affinity, which was better than that of controlled drug ningnanmycin (K<sub>d</sub>=0.52 ± 0.25 µmol/L)  
 121 and lead compound myricetin (K<sub>d</sub>=92.23 ± 47.54 µmol/L). Based on anti-TMV activities and MST  
 122 results, we can predict that the structural modification of the lead compound myricetin, such as the  
 123 introduction of the active groups ferulic acid amide, could greatly improved the antiviral activities.



124

125

126

**Figure 2.** Microscale thermophoresis results of compounds **4l** (A), **4m** (B), myricetin (C) and ningnanmycin (D)

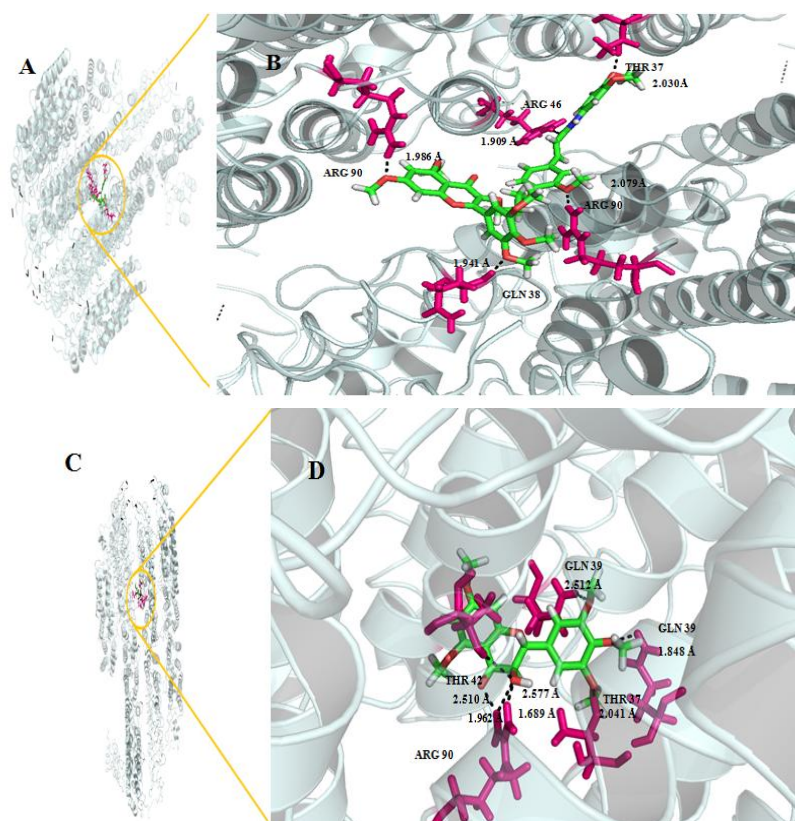


127 **Table 3.** The dissociation constant of **4l**, **4m**, myricetin and ningnanmycin with TMV- CP.

Compounds	$K_i$ ( $\mu\text{mol/L}$ )
<b>4l</b>	$0.34 \pm 0.09$
<b>4m</b>	$2.30 \pm 0.77$
myricetin	$92.23 \pm 47.54$
ningnanmycin	$0.52 \pm 0.25$

128 2.5. Molecular docking of **4l** and myricetin with TMV-CP

129 To identify the **4l** and myricetin recognition sites in TMV-CP (Protein Data Bank (PDB) code:  
 130 1EI7), we performed molecular docking using the gold method with 200 cycles [27, 29, 30]. As was  
 131 shown in the **Figure 3**, the compound **4l** was well-embedded between the two subunits of TMV-CP.  
 132 Previous reports have showed that these residues play key roles in the self-assembly of TMV  
 133 particles[31]. The binding orientation of compound **4l** was clearly shown in **Figure 3**(A and B), it  
 134 forms one hydrogen bond with ARG-46, with the highest docking score (1.909 Å) among the  
 135 designed molecules. Besides, compound **4l** deep into the active pocket formed by amino-acid  
 136 residue, including ARG-90, CLN-38 and THR-37. These interactions between small molecules and  
 137 the TMV-CP may impair the interaction of two TMV-CP subunits, hence preventing self-assembly of  
 138 the TMV particle. As was shown in the **Figure 3**, The hydrogen bond strength of compound **4l**  
 139 was stronger than that of myricetin (C and D). Based on molecular docking results of compound **4l** and  
 140 myricetin, we can predict that the structural modification of the lead compound myricetin, could  
 141 greatly improved the antiviral activities.



142

143

144

**Figure 3** Molecular docking studies of compounds **4l** (A–B) and myricetin (C–D)

### 145 3. Experimental

146 The melting points were determined by X-4B microscopic melting point meter (Shanghai Yi  
147 Dian Physical Optics Instrument Co., Ltd. China); proton nuclear magnetic resonance (NMR) spectra  
148 were obtained on JEOL-ECX500 NMR spectrometer (JEOL, Tokyo, Japan) and Bruker Ascend-400  
149 spectrometer (Bruker, Germany) with DMSO-*d*<sub>6</sub> or CDCl<sub>3</sub> as the solvent and TMS as the internal  
150 standard. High-resolution mass spectral (HRMS) data were performed with Thermo Scientific Q  
151 Exactive (Thermo Scientific, USA ). The micro thermophoresis of the compound and TMV CP was  
152 determined by a micro thermophoresis instrument (NanoTemper Technologies GmbH, Germany);  
153 the fluorescence spectroscopy of the compound interacting with TMV CP was determined by  
154 FluoroMax-4 fluorescence spectrometer (HORIBA Scientific, France). All reagents (analytical grade)  
155 were purchased from commercial suppliers.

#### 156 3.1. Chemistry

##### 157 3.1.1. General synthesis procedure for intermediate 1

158 Ferulic acid (3.01 g, 15.45 mmol) were added into bottom flask and dissolved it by 10 % NaOH  
159 (30 mL), then added acetic anhydride (1.97 g, 19.31 mmol). The mixture was stirred at room  
160 temperature for 1 h. Then added 200 mL H<sub>2</sub>O to the reaction mixture and adjust pH to 4-5 by 10 %  
161 HCl, filtering the mixture and washing the precipitate by H<sub>2</sub>O to obtained the intermediate 1 [16].

##### 162 3.1.2. General synthesis procedure for intermediate 2

163 Intermediate 1 (0.55 g, 2.33 mmol), 1-Hydroxybenzotriazole (0.38 g, 2.79 mmol) and 1-ethyl-3-  
164 (3-dimethylaminopropyl) carbodiimide hydrochloride (0.54 g, 2.79 mmol) were dropped into  
165 acetonitrile (20 mL), the mixture was stirred at room temperature for 3 h. Then acetonitrile (20 mL)  
166 containing substituted aniline (0.27 g, 2.56 mmol) was dropped slowly to the mixture, stirred and  
167 refluxed at 90 °C for 5 h until the reaction was completed (monitor by TLC:  $V_{ethyl\ acetate} : V_{methanol} = 10:1$ ).  
168 Then the reaction mixture was extracted by ethyl acetate and evaporated under reduced pressure.  
169 The product was dissolved in acetonitrile again, added hydrazine hydrate (0.24 g, 4.66 mmol), and  
170 stirred at room temperature for 2 h to obtained the intermediate 2 [19, 24].

##### 171 3.1.3. General synthesis procedure for intermediate 3

172 Preparation of the intermediate 3 has been previously described [23, 32]. The mixture of  
173 myricitrin (0.55 g, 5.01 mmol), CH<sub>3</sub>I (2.02 g, 60.02 mmol), and K<sub>2</sub>CO<sub>3</sub> (0.19 g, 6.13 mmol) was  
174 dissolved in *N,N*-dimethyl formamide (DMF; 30 mL), and stirred at 40 °C for 2 d until the reaction  
175 was complete (as indicated by TLC analysis). The reaction mixtures were then filtered, and the  
176 filtrate was dissolved in 50 mL water and finally extracted three times with dichloromethane (30  
177 mL×3), combined the dichloromethane and concentrated under reduced pressure. The concentrated  
178 solution was diluted with 20 mL of absolute ethanol, stirred, and refluxed for 1 h. The concentrated  
179 hydrochloric acid (3 mL) was slowly added to the above obtained, for 2 h in reflux. The solid was  
180 precipitated from the clear solution. After cooling to room temperature, the reaction mixture was  
181 filtered, and the obtained solid product was dried at 40 °C for 2 h. Finally, dibromoalkanes and  
182 DMF were added reflux 6h to obtained intermediate 3.

183 3.1.4. General synthesis procedure for target compound **4a–4v**.

184 A mixture of intermediate **2** (0.31 g, 1.08 mmol), anhydrous K<sub>2</sub>CO<sub>3</sub> (0.41 g, 2.94 mmol) in DMF  
 185 (30 mL) was stirred at 85 °C for 1 h, then DMF (20 mL) containing intermediate **3** (0.50 g, 0.98 mmol)  
 186 was dropped slowly to the mixture and reacted at 105 °C for 6 h. After cooling to the room  
 187 temperature, the reaction mixture was added about 200 mL H<sub>2</sub>O and adjusted pH to 4-5 by 10 %  
 188 HCl, filtered and washed by H<sub>2</sub>O. Finally, compounds **4** was gained by re-crystallization from  
 189 methanol.

190 (E)-3-(4-(3-((5,7-dimethoxy-4-oxo-2-(3,4,5-trimethoxyphenyl)-4H-chromen-3-yl)oxy)propoxy)-3-  
 191 methoxyphenyl)-N-(p-tolyl)acrylamide (**4a**): gray solid, m. p. 215.4-215.5, yield: 58.68 %, <sup>1</sup>H NMR  
 192 (400 MHz, CDCl<sub>3</sub>) δ 8.01 (s, 1H, NH), 7.63 (t, J = 11.8 Hz, 1H, Ph-H), 7.57 (d, J = 7.1 Hz, 2H, Ph-2H),  
 193 7.32 (s, 2H, Ph-2H), 7.13 (d, J = 8.2 Hz, 2H, Ph-2H), 7.00 (d, J = 8.3 Hz, 1H, CO-CH=CH), 6.95 (s, 1H,  
 194 Ph-H), 6.74 (d, J = 8.3 Hz, 1H, Ph-H), 6.51 (d, J = 2.1 Hz, 1H, Ph-H), 6.47 (s, 1H, CO-CH=), 6.36 (d, J =  
 195 2.2 Hz, 1H, Ph-H), 4.23 (t, J = 5.9 Hz, 2H, CH<sub>2</sub>), 4.18 (t, J = 6.7 Hz, 2H, CH<sub>2</sub>), 3.94 (s, 3H, OCH<sub>3</sub>), 3.92  
 196 (d, J = 3.4 Hz, 6H, 2×OCH<sub>3</sub>), 3.88 (s, 6H, 2×OCH<sub>3</sub>), 3.77 (s, 3H, OCH<sub>3</sub>), 2.31 (d, J = 9.9 Hz, 3H, CH<sub>3</sub>),  
 197 2.25 (dd, J = 12.6, 6.3 Hz, 2H, CH<sub>2</sub>), <sup>13</sup>C NMR (101 MHz, CDCl<sub>3</sub>) δ 174.07, 164.12, 163.82, 160.99,  
 198 158.83, 153.02, 152.77, 150.00, 149.22, 141.68, 140.56, 140.00, 129.51, 127.77, 125.94, 121.78, 119.88,  
 199 112.61, 110.41, 109.35, 105.91, 95.89, 92.49, 69.26, 66.00, 61.01, 56.38, 56.30, 55.86, 55.77, 30.13, 20.91,  
 200 HRMS calcd for C<sub>40</sub>H<sub>41</sub>NO<sub>11</sub>[M+H]<sup>+</sup>: 712.2753, found 712.2752.

201 3.2. Antiviral activities *in vitro*

202 3.2.1. Purification of TMV

203 The upper leaves of *N. tabacum* cv. K<sub>326</sub> were selected and inoculated with TMV, using  
 204 previously reported methods for TMV purification[33].

205 3.2.2. Curative activity of the target compounds against TMV *in vivo*

206 Growing *N. tabacum* L. leaves of the same age were selected. The leaves were inoculated with  
 207 TMV (concentration of 6×10<sup>-3</sup> mg/mL) by dipping and brushing the whole leaves, which had  
 208 previously been scattered with silicon carbide. The leaves were then washed with water after  
 209 inoculation for 0.5 h. The compound solution was smeared on the left side of the leaves, and the  
 210 solvent was smeared on the right side as the control. The number of local lesions was counted and  
 211 recorded 3–4 d after inoculation. Three replicates were set up for each[25, 26].

212 3.2.3. Protection activity of the target compounds against TMV *in vivo*

213 The compound solutions were smeared on the left side of the *N. tabacum* L. leaves, and the  
 214 solvents were smeared on the right side as the control sample for growing *N. tabacum* L. leaves. After  
 215 12 h, crude TMV (concentration of 6×10<sup>-3</sup> mg/mL) was inoculated on whole leaves at the same  
 216 concentration on each side of the leaves, which were previously scattered with silicon carbide. After  
 217 0.5 h, the leaves were washed with water and then dried. The number of local lesions was recorded  
 218 3–4 d after inoculation[25, 26]. Three replicates were used for each compound. The inhibitory rate  
 219 (*I* %) of the compound was calculated according to the following formula:

$$220 (I \%) = (C_{\text{num}} - T_{\text{num}}) / C_{\text{num}} \times 100 \%$$

221 *T*<sub>num</sub>: average local lesion number smeared with drugs



222  $C_{num}$ : average local lesion number of control(not treated with compounds)

### 223 3.3 Expression and purification of TMV-CP

224 The expression vector, pET28a-TMV-CP, containing the full-length TMV-CP gene, was stored at  
225 -80 °C in our lab. A freshly transformed overnight culture of *Escherichia coli* strain BL21(DE3)  
226 containing the plasmid pET28a-TMV-CP was transferred to 1L Luria broth. The cells were grown at  
227 37 °C in Luria-Bertani medium supplemented with 50 µg/mL kanamycin, and with an OD<sub>600</sub> of 0.8.  
228 The cells were shaken at 200 rpm. Then protein expression was induced with 0.8 mmol IPTG at 16 °C  
229 overnight. The cells were harvested by centrifugation and then stored at -80 °C. When analyzed, the  
230 cells were resuspended in lysis buffer (20 mmol PB, 500 mmol NaCl, 30 mmol imidazole, 5 mmol  
231 β-mercaptoethanol and 5 % glycerol, pH=7.2) and then lysed at 4 °C by sonication. The lysate was  
232 clarified by centrifugation at 12,000 g for 30 min at 4 °C, the soluble supernatants were loaded onto a  
233 5 mL Ni-NTA column (GE Healthcare, USA), and the protein was eluted with a linear gradient of  
234 30-350 mmol imidazole (pH=7.2). The crude protein was performed at 4 °C using a desalting column  
235 (GE Healthcare, USA) attached to an AKTA purifier protein liquid chromatography system (GE  
236 Healthcare, USA), and the fractions containing target protein with His-tags were pooled,  
237 concentrated to a suitable concentration by ultrafiltration (10 kDa cut-off). The dealt protein  
238 concentration was determined using a Genequant 100 (GE Healthcare, USA), and stored at -80 °C  
239 until further analysis [27-29].

### 240 3.4. Interaction studies between 4I or myricetin and TMV-CP

241 The binding was calculated for MST Monolith NT. 115 (Nano Temper Technologies, Germany).  
242 A range of ligands from 0 to 5 µmol were incubated with 0.5 µmol of purified recombinant proteins  
243 for 5 min with a NT-647 dye (Nano Temper Technologies, Germany) and was used in the  
244 thermophoresis experiment at a final concentration of 20 µmol. A 16 point dilution series was made  
245 for selected compounds in DMSO. Each compound dilution series was subsequently transferred to  
246 protein solutions in 10 µmol Tris-HCl and 100 mmol sodium chloride pH=7.5, 0.05 % Tween-20.  
247 After a 15 min incubation of the labeled TMV-CP with each dilution point (1:1 mix) at room  
248 temperature, samples were filled into standard capillaries (NanoTemper Technologies, Germany).  
249 Measurements were taken on a Monolith NT.115 microscale thermophoresis system (NanoTemper  
250 Technologies, Germany) under a setting of 20 % LED and 40 % IR laser. Laser on time was set at 30 s,  
251 and laser-off time was set at 5 s. The  $K_d$  values were calculated from the duplicate reads of three  
252 separate experiments using the mass action equation in the Nano Temper software[28].

### 253 3.5. Molecular docking

254 The molecular docking was performed by using DS-CDocker implemented in Discovery Studio  
255 (version 4.5). The coat protein subunit amino acid sequence of tobacco mosaic virus (TMV) was  
256 searched by the UniProt database. The Protein BLAST server was used to search the template  
257 protein and the homologies of TMV-CP sequences were aligned. Homology modeling of TMV-CP  
258 was carried out using Create Homology Models, which is a module integrated in Discovery Studio.  
259 The obtained models were evaluated by Ramachandran plots. The 3D structures of the compounds  
260 were constructed using the Sketching module and optimized by the Full Minimization module. All  
261 parameters are default during the docking process[27, 29, 30].

## 262 4. Conclusions

263 A series of myricetin derivatives bearing ferulic acid amide scaffolds were designed and  
 264 synthesized. Preliminary bioassays suggested that these compounds exhibited favorable curative  
 265 and protective activities against TMV. Among them, compound **41** showed remarkable protective  
 266 activity against TMV, with the EC<sub>50</sub> values of 196.11 µg/mL, which was superior to ningnamycin  
 267 (447.92 µg/mL). Further the microscale thermophoresis studies revealed that compound **41** have  
 268 strong binding capability with TMV-CP, and the molecular docking studies were consistent with  
 269 the experimental results. All these results support that the myricetin derivatives bearing ferulic acid  
 270 amide scaffolds possess antiviral activities, and thus could be further studied as potential  
 271 alternative templates in the search for novel antiviral agents.

272 **Supplementary Materials:** The following are available online. The data and spectrogram of compounds **4a–4v**.

273 **Acknowledgments:** The authors gratefully acknowledge grants from the National Key R & D Program of  
 274 China (No. 2017YFD0200506), the National Nature Science Foundation of China (No. 21867003), Science Fund  
 275 of Guizhou, China (Nos. 20191105, 20185781).

276 **Author Contributions:** Wei Xue conceived and designed the experiments. Xu Tang and Cheng Zhang  
 277 performed the experiments and analyzed the data; Mei Chen and Yining Xue evaluated the antiviral activities  
 278 of the title compounds. Tingting Liu provided the material for evaluating the antiviral activities. All authors  
 279 contributed to this study, read and approved the final manuscript.

280 **Conflicts of Interest:** The authors declare no conflict of interest.

## 281 References

- 282 1. Chen, L.J.; Xia, R.J.; Tang, X.; Chen, Y.; Zhang, C.; Xue, W. Novel Phosphorylated Penta-1,4-dien-3-one  
 283 Derivatives: Design, Synthesis, and Biological Activity[J]. *Molecules*, **2019**, *24*, 925.
- 284 2. Wang, P.Y.; Zhou, L.; Zhou, J.; Wu, Z.B.; Xue, W.; Song, B.A.; Yang, S. Synthesis and antibacterial activity  
 285 of pyridinium-tailored 2,5-substituted-1,3,4-oxadiazole thioether/ sulfoxide/sulfone derivatives[J]. *Bioorg.*  
 286 *Med. Chem. Lett.* **2016**, *26*, 1214–1217.
- 287 3. Gan, X.H.; Hu, D.Y.; Li, P.; Wu, J.; Chen, X.W.; Xue, W.; Song, B.A. Design, synthesis, antiviral activity  
 288 and three-dimensional quantitative structure-activity relationship study of novel 1,4-pentadien-3-one  
 289 derivatives containing the 1,3,4-oxadiazole moiety[J]. *Pest Manag. Sci.* **2016**, *72*, 534–543.
- 290 4. Qian, X.H.; Lee, P.W.; Song, C. China: Forward to the Green Pesticides via a Basic Research Program[J]. *J.*  
 291 *Agric. Food Chem.* **2010**, *58*, 2613–2623.
- 292 5. Leonard, G.C.; Stephen, O.D. Natural products that have been used commercially as crop protection  
 293 agents[J]. *Pest Manag Sci.* **2007**, *63*, 524–554.
- 294 6. Marrone, P.G. Microbial pesticides and natural products as alternatives[J]. *Out Look AGR.* **1999**, *28*,  
 295 149–154.
- 296 7. Sultana, B.; Anwar, F. Flavonols (kaempferol, quercetin, myricetin) contents of selected fruits,  
 297 vegetables and medicinal plants[J]. *Food Chem.* **2008**, *108*, 879–884.
- 298 8. Tong, Y.; Zhou, X.M.; Wang, S.J.; Yang, Y.; Cao, Y.L. Analgesic activity of myricetin isolated from *Myrica*  
 299 *rubra* Sieb. et Zucc. leaves[J]. *Arch Pharm Res.* **2009**, *32*, 527–533.
- 300 9. Wang, X.R.; Wang, Z.Q.; Li, Y. Studies on the chemical constituents of *Abelmoschus manihot* L. Medic[J].  
 301 *Acta Botanica Sinica.* **1981**, *23*, 222–227.
- 302 10. Lee, K.W.; Kang, N.J.; Rogozin, E.A.; Kim, H.G.; Cho, Y.Y.; Bode, A.M.; Joo, H.; Surh, Y.J.; Bowden, G.T.;  
 303 Dong, Z. Myricetin is a novel natural inhibitor of neoplastic cell transformation and MEK1[J].  
 304 *Carcinogenesis*, **2007**, *28*, 1918–1927.

- 305 11. Su, X.W.; D'Souza, D.H. Naturally occurring flavonoids against human norovirus surrogates[J]. *Food*  
306 *Environ Virol* . **2013**, *5*, 97–102.
- 307 12. Zhong, X.M.; Wang, X.B.; Chen, L.J.; Ruan, X.H.; Li,Q.; Zhang, J.P.; Chen, Z.; Xue, W. Synthesis and  
308 biological activity of myricetin derivatives containing 1,3,4-thiadiazole scaffold[J]. *Chem. Cent. J.*  
309 **2017**,*11*,106.
- 310 13. Chen, C.C.; Huang, C.Y. Inhibition of *Klebsiella Pneumoniae* DnaB Helicase by the Flavonol Galangin[J].  
311 *Protein J.* **2011**, *30*, 59–65.
- 312 14. Rashed, K.; Ćirić, A.; Glamočlija, J.; Soković, M. Antibacterial and antifungal activities of methanol  
313 extract and phenolic compounds from *Diospyros virginiana* L[J]. *Ind. Crop. Prod.* **2014**, *59*, 210–215.
- 314 15. Chobot, V.; Hadacek, F. Exploration of pro-oxidant and antioxidant activities of the flavonoid  
315 myricetin[J]. *Redox. Rep.* **2011**, *16*, 242–247.
- 316 16. Xue, W.; Song, B.A.; Zhao, H.J.; Qi, X.B.; Huang, Y.J.; Liu, X.H. Novel myricetin derivatives: Design,  
317 synthesis and anticancer activity[J]. *Eur. J. Med. Chem.* **2015**, *97*, 155–163.
- 318 17. Ha, T.K.; Jung, I.; Kim, M.E.; Bae, S.K.; Lee, J.S. Anti-cancer activity of myricetin against human papillary  
319 thyroid cancer cells involves mitochondrial dysfunction-mediated apoptosis[J]. *Biomed. Pharmacother.*  
320 **2017**, *91*, 378–384.
- 321 18. Ou, S.; Kwok, K.C. Ferulic acid: pharmaceutical functions, preparation and applications in foods[J]. *J. Sci.*  
322 *Food Agric.* **2004**, *84*, 1261–1269.
- 323 19. Wu, Z.X.; Zhang, J.; Chen, J.X.; Pan, J.K.; Zhao, L.; Liu, D.Y.; Zhang, A.W.; Chen, J.; Hu,D.Y.; Song, B.A.  
324 Design, synthesis, antiviral bioactivity and three-dimensional quantitative structure–activity relationship  
325 study of novel ferulic acid ester derivatives containing quinazoline moiety[J]. *Pest Manag. Sci.* **2017**, *73*,  
326 2079–2089.
- 327 20. Shi, Y.G.; Wu, Y.; Lu, X.Y.; Ren, Y.P.; Wang, Q.; Zhu, C.M.; Yu, L.; Wang, H. Lipase-catalyzed  
328 esterification of ferulic acid with lauryl alcohol in ionic liquids and antibacterial properties *in vitro*  
329 against three food-related bacteria[J]. *Food Chem.* **2017**, *220*, 249–256.
- 330 21. Eroğlu, C.; Seçme, M.; Bağcı, G.; Dodurga,Y. Assessment of the anticancer mechanism of ferulic acid via  
331 cell cycle and apoptotic pathways in human prostate cancer cell lines[J]. *Tumor biology.* **2015**, *36*,  
332 9437–9446.
- 333 22. Kumar, N.; Kumar, S.; Abbat, S.; Nikhil, K.; Sondhi, S. M.; Bharatam, P. V.; Roy, P.; Pruthi, V. Ferulic acid  
334 amide derivatives as anticancer and antioxidant agents: synthesis, thermal, biological and computational  
335 studies[J]. *Med. Chem. Res.* **2016**, *25*, 1175–1192.
- 336 23. Liu, H.R.; Liu, L.B.; Gao, X.H.; Liu, Y.Z.; Xu,W.J.; He,W.; Jiang, H.; Tang, J.J.; Fan, H.Q.; Xia, X.H. Novel  
337 ferulic amide derivatives with tertiary amine side chain as acetylcho linesterase and  
338 butyrylcholinesterase inhibitors: The influence of carbon spacer length, alkylamine and aromatic  
339 group[J]. *Eur. J. Med. Chem.* **2017**,*126*, 810–822.
- 340 24. Chen, J.X.; Chen, Y.Z.; Gan, X.H.; Song, B.J.; Hu, D.Y.; Song, B.A. Synthesis, Nematicidal Evaluation, and  
341 3D-QSAR Analysis of Novel 1,3,4-Oxadiazole–Cinnamic Acid Hybrids[J]. *J. Agric. Food Chem.* **2018**, *66*,  
342 9616–9623.
- 343 25. Chen, J.; Shi, J.; Yu, L.; Liu, D.; Gan, X.H.; Song, B.A.; Hu, D.Y. Design, synthesis, antiviral bioactivity  
344 and defense mechanisms of novel dithioacetal derivatives bearing a strobilurin moiety[J]. *J. Agric. Food*  
345 *Chem.* **2018**, *66*, 5335–5345.
- 346 26. Wu, Z.X.; Zhang, J.; Chen, J.X.; Pan, J.K.; Zhao, L.; Liu, D.Y.; Zhang, A.W.; Chen, J.; Hu, D.Y.; Song, B.A.  
347 Design, synthesis, antiviral bioactivity and three-dimensional quantitave structure-activity relationship  
348 study of novel ferulic acid ester derivatives containing quinazoline moiety[J]. *Pest Manag. Sci.* **2017**, *73*,  
349 2079–2089.
- 350 27. Li, X.Y.; Liu, J.; Yang, X.; Ding, Y.; Wu, J.; Hu, D.Y.; Song, B.A. Studies of binding interactions between  
351 dufulin and southern rice black-streaked dwarf virus P9-1[J]. *Bioorg. Med. Chem.* **2015** , *23*, 3629–3637.

- 352 28. Wienken, C.J.; Baaske, P.; Rothbauer, U.; Braun, D.; Duhr, S. Protein-binding assays in biological liquids  
353 using microscale thermophoresis[J]. *Nat. Commun.* **2010**, *1*, 100.
- 354 29. Chen, L.J.; Guo, T.; Xiao, R.J.; Tang, X.; Chen, Y.; Zhang, C.; Xue, W. Novel Phosphorylated  
355 Penta-1,4-dien-3-one Derivatives: Design, Synthesis, and Biological Activity[J]. *Molecules*, **2019**, *24*, 925.
- 356 30. Tang, X.; Su, S.J.; Chen, M.; He, J.; Xia, R.J.; Guo, T.; Chen, Y.; Zhang, C.; Wang, J.; Xue, W. Novel chalcone  
357 derivatives containing a 1,2,4-triazine moiety: design, synthesis, antibacterial and antiviral activities[J].  
358 *RSC Adv.* **2019**, *9*, 6011–6020.
- 359 31. Bloomer, A. C.; Champness, J. N.; Bricogne, G. Protein disk of tobacco mosaic virus at 2.8 Å resolution  
360 showing the interactions within and between subunits[J]. *Nature*, **1978**, *276*, 362–368.
- 361 32. Ruan, X.H.; Zhao, H.J.; Zhang C.; Chen, L.J.; Li, P.; Wang Y.H.; He, M.; Xue, W. Syntheses and  
362 Bioactivities of Myricetin Derivatives Containing Piperazine Acidamide Moiety[J]. *Chem. J. Chinese U.*  
363 **2018**, *39*, 1197–1204.
- 364 33. Gooding, G.V.J.; Hebert, T.T. A simple technique for purification of tobacco mosaic virus in large  
365 quantities[J]. *Phytopathology*, **1967**, *57*, 1285.